RSC Advances

PAPER

View Article Online
View Journal | View Issue

Cite this: *RSC Adv.*, 2017, **7**, 36807

A green approach to the synthesis of Ag doped nano magnetic γ-Fe_2O_3@SiO_2-CD core–shell hollow spheres as an efficient and heterogeneous catalyst for ultrasonic-assisted A^3 and KA^2 coupling reactions†

S. Sadjadi,*[a] M. Malmir[b] and M. M. Heravi *[b]

Using a green approach and ultrasonic-assisted template-free five-step process, a novel heterogeneous catalyst, γ-Fe_2O_3@SiO_2-CD/Ag hollow spheres (h-Fe_2O_3@SiO_2-CD/Ag), was fabricated. The design of the catalyst was based on the synthesis of core–shell h-Fe_2O_3@SiO_2 followed by amine functionalization, reaction with tosylated cyclodextrin and subsequent Ag(0) doping using hollyhock flowers collected from the Banaruiyeh District, in Larestan, Iran as extract-based reducing agent. The novel catalyst was fully characterized using SEM/EDX, BET, TGA, ICP-AES, FTIR, VSM and XRD techniques. The hybrid catalyst was successfully applied for promoting A^3 and KA^2 coupling reactions under mild and green conditions, *i.e.* ultrasonic irradiation at room temperature in aqueous media. Studying the reusability of the catalyst and Ag(0) nanoparticle leaching established that the catalyst can be recovered and reused with preserving its catalytic activity and negligible Ag(0) leaching for five reaction runs. Upon reusing for the sixth run, however, slight leaching of Ag(0) and consequently loss of catalytic activity was observed.

Received 25th April 2017
Accepted 20th July 2017

DOI: 10.1039/c7ra04635a

rsc.li/rsc-advances

Introduction

Propargylamine derivatives are key intermediates which are broadly applied for the synthesis of a diverse range of natural products and biologically active nitrogen containing chemicals such as herbicides, fungicides, restricted peptide isosteres, oxotremorine analogues, indolizines, pyrroles and quinolines.[1–4] Propargylamines can be obtained from three-component coupling reaction of amines, aldehydes and alkynes, referred to as the A^3 coupling reaction. Using this valuable one-pot procedure several elements can be introduced into a molecule.[5] This reaction can be promoted by using various metal catalysts such as gold, copper, iron, silver and zinc based catalysts[3,6,7] that are able to activate the terminal C–H bond of the alkyne. Despite developing some promising methodologies, some of them require a toxic solvent such as toluene, or expensive media, like ionic liquids.[8] Therefore, development of a novel, efficient and heterogeneous catalyst for this process is of great interest.

Magnetic nanoparticles, MNPs, and its core–shell structures received ongoing interest due to their outstanding properties such as high magnetic susceptibility and coercivity, super paramagnetic behaviour and high surface area.[9] This class of materials has been widely used for catalysis, target-drug delivery, hyperthermia treatment of cancer, diagnosis, MRI, enzyme immobilization, magnetic separation and sensors.[10–12] Among various uses, catalysis has gained growing interest. Using MNPs diverse range of heterogeneous catalysts with tuneable size and morphologies can be designed and synthesized. Another merit of MNPs is their facile separation from the reaction mixture, which is more efficient and economical than conventional filtration and centrifuge approaches.[13–15]

Hollow MNPs (h-MNPs), benefit from high surface areas, tiny particle sizes and low densities. However, they may suffer from aggregations. To circumvent this issue, the surface of h-MNPs is usually decorated with stabilizing agents.[14]

Ultrasonic irradiation is a useful tool for developing green and clean procedures for the synthesis of organic compounds. The notable advantageous of ultrasonic-assisted approaches are accelerated reaction rates, waste minimizing, and simplicity of the procedure, high yields and purities of products.[16,17] The effect of ultrasonic irradiation can be defined on the base of cavitation effect. The ultrasonic irradiation can cause high local

[a]*Gas Conversion Department, Faculty of Petrochemicals, Iran Polymer and Petrochemical Institute, PO Box 14975-112, Tehran, Iran. E-mail: samahesadjadi@yahoo.com*

[b]*Department of Chemistry, School of Science, Alzahra University, PO Box 1993891176, Vanak, Tehran, Iran. E-mail: mmh1331@yahoo.com; mmheravi@alzahra.ac.ir; Fax: +98 21 88041344; Tel: +98 21 88044051*

† Electronic supplementary information (ESI) available. See DOI: 10.1039/c7ra04635a

temperatures and pressure inside the bubbles and accelerates mass transfer and turbulent flow in the liquid.[17]

In last decade, we devoted our research to develop new heterogeneous and reusable catalysts for promoting organic transformations.[14,18–22] In continuation of our attempts, herein, we wish to disclose a novel efficient hybrid catalyst for promoting A^3 and KA^2 coupling reactions under mild and green reaction condition. The design of the catalyst is based on fabrication of γ-Fe_2O_3 hollow spheres, which we disclosed in our previous report,[14] followed by formation of SiO_2 shell. The obtained h-Fe_2O_3@SiO_2 was subsequently amine functionalized with 3-*N*-(2-(trimethoxysilyl)ethyl)methanediamine and reacted with tosylated cyclodextrin to form h-Fe_2O_3@SiO_2-CD. The latter was then doped with Ag(0) NPs by using hollyhock flower extract as a extract-based reducing agent (Scheme 1). The reusability and Ag(0) leaching were also studied. Moreover, the catalytic performance of the catalyst was compared with some of previously reported catalytic procedures.

Results and discussion

Catalyst characterization

To confirm the formation of h-Fe_2O_3@SiO_2-CD/Ag, the FTIR spectrum of the catalyst was obtained and compared with h-Fe_2O_3@SiO_2-CD, Fig. 1. The strong absorption bands observed at 470–590 cm^{-1} can be assigned to Fe–O stretching vibration and confirm the formation of magnetic NPs.[14] Both spectra exhibited the characteristic band of Si–O stretching at 1082 cm^{-1} indicating the successful coverage of SiO_2 shell. The absorption peaks at 980, 810 and 470 cm^{-1} were in good agreement with the bending vibrations of the Si–O–Si bond.[9] The bands at 2925 cm^{-1} and 3493 cm^{-1} can be attributed to the

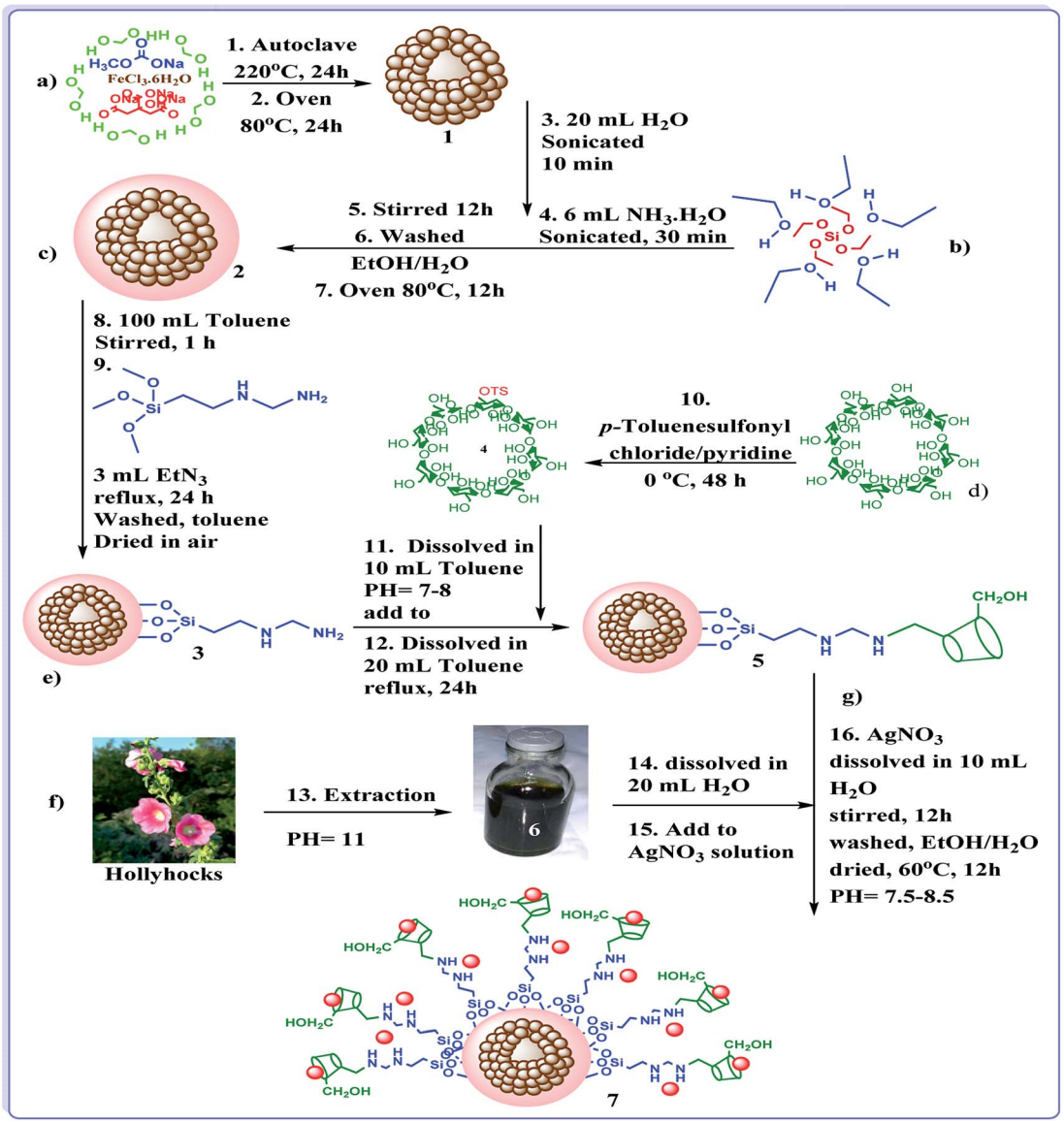

Scheme 1 The possible formation process of h-Fe_2O_3@SiO_2-CD/Ag hollow spheres.

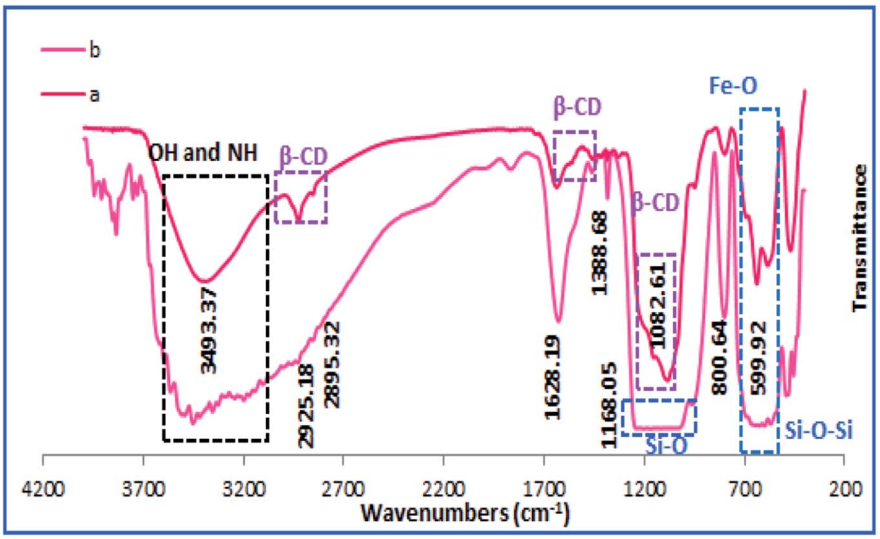

Fig. 1 The FT-IR spectra of (a) h-Fe_2O_3@SiO_2-CD and (b) h-Fe_2O_3@SiO_2-CD/Ag.

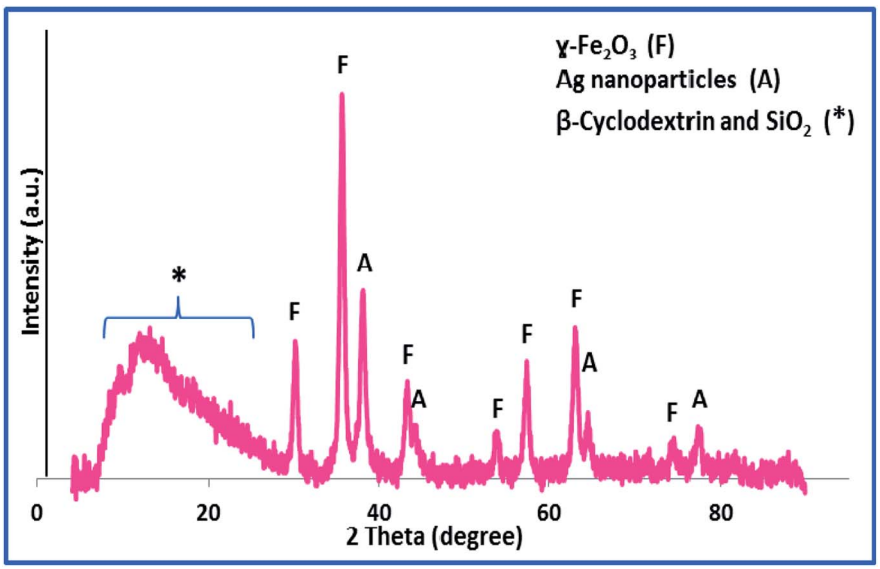

Fig. 2 The XRD pattern of h-Fe_2O_3@SiO_2-CD/Ag.

–CH_2 stretching and –NH functionality and prove the conjugation of 3-*N*-(2-(trimethoxysilyl)ethyl)methanediamine.

These bands can also represent the –OH and –CH_2 groups in CD. Comparing the FTIR spectra of h-Fe_2O_3@SiO_2-CD and h-Fe_2O_3@SiO_2-CD/Ag reveals the broadening and sharpening of the bands upon Ag incorporation. According to the previous reports,[23] biological extracts contain several functional groups that can be clearly detected in FTIR analysis. Hence the broadening and sharpening of the bands in and h-Fe_2O_3@SiO_2-CD/Ag can be assigned to the presence of some functionalities in hollyhock flower extract such as –OH, C=N, N–H, C–H *etc.*

The X-ray diffraction pattern, XRD, was exploited for investigation of the phase and composition of h-Fe_2O_3@SiO_2-CD/Ag, Fig. 2. According to the literature,[24] the broad halo observed at 2θ = 3–20 (labelled as *) can be assigned to the amorphous silica and CD. Moreover, the observed peaks at 30.3, 35.6, 43.2, 54.0, 57.3, 63.0 and 74.6 (labelled as F) can be attributed to the {220}, {311}, {400}, {422}, {511}, {440} and {533} planes of the typical cubic structure hematite (γ-Fe_2O_3) (JCPDS card no. 39-1346).[14] The peaks labelled as A are characteristic peaks of Ag(0) NPs (JCPDS card no. 04-0783). Using Debye–Scherrer equation, the average particle size of Ag(0) NPs was estimated to be 37 nm.

To provide more insight into the properties of the catalyst, thermo gravimetric analysis (TGA) of h-Fe_2O_3@SiO_2-CD/Ag was carried out, Fig. 3. Two degradation steps can be detected for h-Fe_2O_3@SiO_2-CD/Ag over the range of 40–800 °C. The first weight loss, observed at about 180 °C, is due to loss of adsorbed water molecules and/or surface hydroxyl groups. The second weight

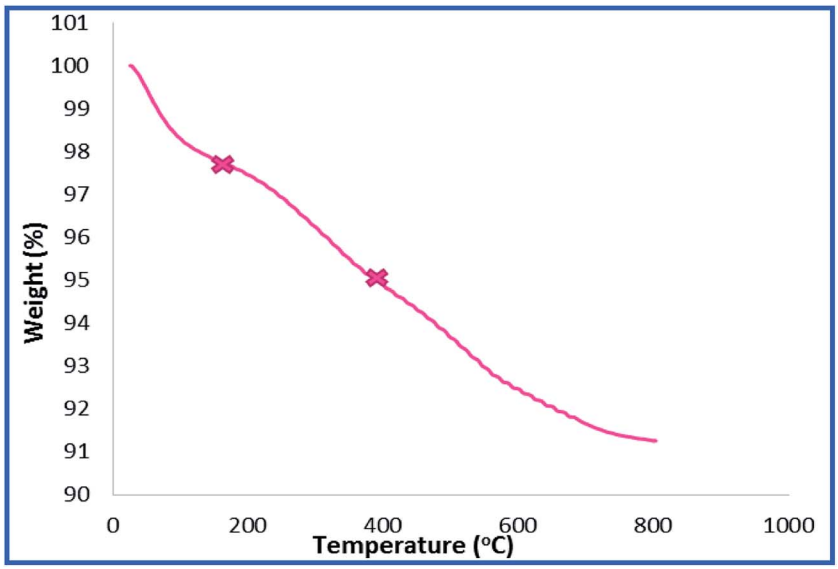

Fig. 3 The TGA analysis of the h-Fe_2O_3@SiO_2-CD/Ag.

loss can be assigned to the degradation of organic moiety. Using TGA analysis, the content of organic moiety in h-Fe_2O_3@SiO_2-CD/Ag was estimated to be about 4 w/w%. To study the morphology of the catalyst and investigating the effect of attachment of 3-*N*-(2-(trimethoxysilyl)ethyl)methanediamine, CD and embedding Ag(0) NPs on the morphology, the FE-SEM analysis of h-Fe_2O_3@SiO_2 and SEM analyses of h-Fe_2O_3@SiO_2-CD and h-Fe_2O_3@SiO_2-CD/Ag were obtained, Fig. 4. As expected, the h-Fe_2O_3@SiO_2 possessed a spherical morphology. Both h-Fe_2O_3@SiO_2-CD and h-Fe_2O_3@SiO_2-CD/Ag exhibited spherical morphologies, indicating that functionalization of h-Fe_2O_3@SiO_2 with CD and incorporation of Ag(0) NPs did not alter the morphology dramatically.

The EDX analysis of h-Fe_2O_3@SiO_2-CD/Ag is shown in Fig. 4d. The presence of the Fe and O atoms can represent the γ-Fe_2O_3 magnetic NPs. Moreover, observation of the Si and O atoms can prove the existence of SiO_2 shell. The conjugation of 3-*N*-(2-(trimethoxysilyl)ethyl)methanediamine and CD can be

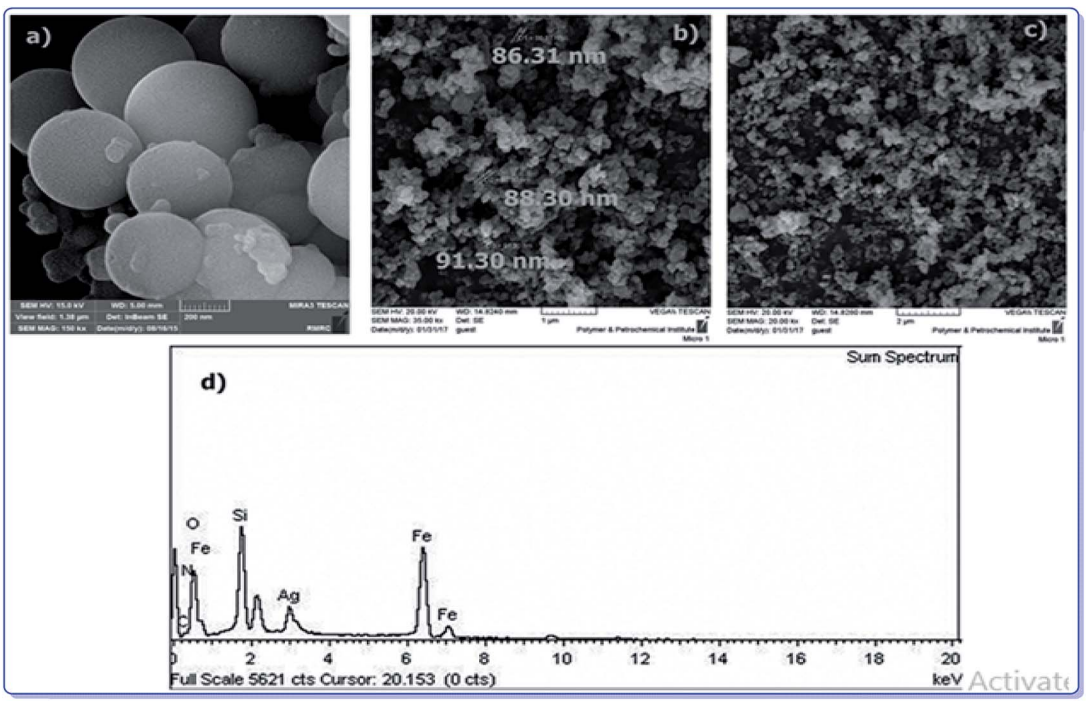

Fig. 4 The FE-SEM analysis of (a) h-Fe_2O_3@SiO_2 and SEM analyses of (b) h-Fe_2O_3@SiO_2-CD, (c) h-Fe_2O_3@SiO_2-CD/Ag and (d) the EDX analysis of h-Fe_2O_3@SiO_2-CD/Ag.

confirmed by the presence of N, Si, C and C and O elements, respectively. The existence of Ag atom in EDX analysis can indicate the incorporation of Ag.

The elemental mapping analysis of h-Fe_2O_3@SiO_2-CD/Ag is illustrated in Fig. 5. As obvious, the N has been distributed uniformly in the catalyst, indicating that 3-*N*-(2-(trimethoxysilyl) ethyl)methanediamine decorated the whole surface of the h-Fe_2O_3@SiO_2–N_2 surface evenly. The good dispersion of Ag NPs also established that Ag(0) NPs were dispersed all around the catalyst.

To disclose the textural properties of the catalyst, the nitrogen adsorption–desorption isotherm of the h-Fe_2O_3@SiO_2-CD/Ag was obtained, Fig. 6. The shape of the isotherm confirmed the porous structure and according to IUPAC classification exhibits type II nitrogen adsorption–desorption isotherms with H3 hysteresis loops.[25] The textural properties including specific surface area, total pore volume and average pore diameter of h-Fe_2O_3@SiO_2-CD/Ag are reported in Table 1. Additionally, these parameters were compared with those of h-Fe_2O_3@SiO_2-CD to investigate the influence of incorporation of Ag(0) doping on the textural properties of final catalyst. Comparison of these parameters established that doping of Ag(0) NPs increased the specific surface area and total pore volume while decreased average pore diameter. According to the previous reports, the increase in specific surface area can emerge from the presence of Ag(0) NPs on h-Fe_2O_3@SiO_2-CD.[26]

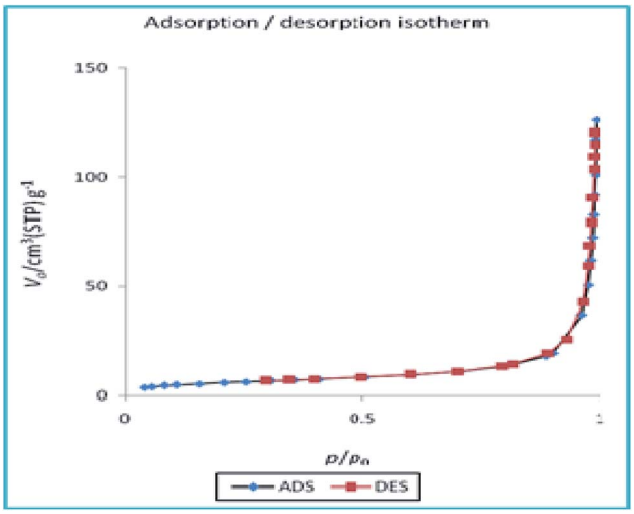

Fig. 6 N_2 adsorption–desorption isotherms of the catalyst.

Using room temperature vibrating sample magnetometer (VSM), the magnetic property of h-Fe_2O_3@SiO_2-CD/Ag was studied and compared with that of h-Fe_2O_3 Fig. 7. As depicted, the maximum saturation magnetization (M_s) value of h-Fe_2O_3@SiO_2-CD/Ag was calculated as 41.15 emu g^{-1} that is slightly lower than M_s of h-Fe_2O_3 (45.28 emu g^{-1}).

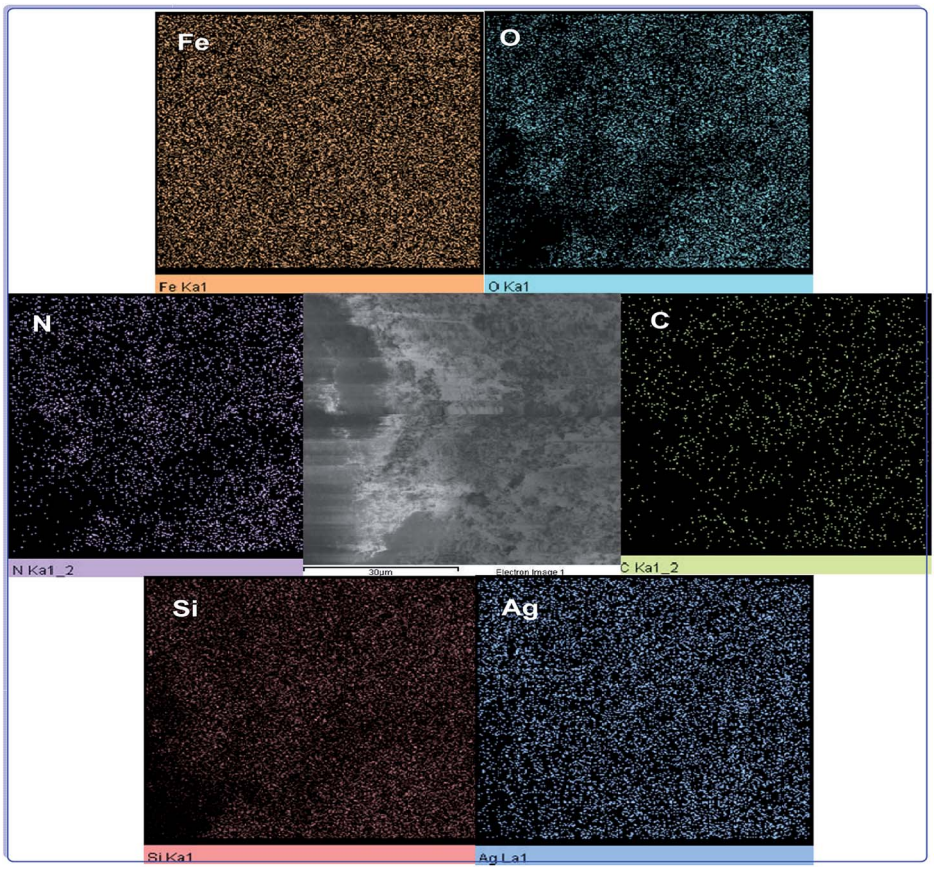

Fig. 5 The elemental mapping analysis of h-Fe_2O_3@SiO_2-CD/Ag.

Table 1 Textural property of the h-Fe_2O_3@SiO_2-CD/Ag and h-Fe_2O_3@SiO_2-CD

Sample	S_{BET} ($m^2\ g^{-1}$)	Total pore volume ($cm^3\ g^{-1}$)	Average pore diameter (nm)
h-Fe_2O_3@SiO_2-CD/Ag	21.067	0.1834	34.822
h-Fe_2O_3@SiO_2-CD	12.139	0.1143	37.679

This result implies that the functionalization of h-Fe_2O_3 and subsequent attachment of CD and incorporation of Ag(0) NPs did not affect the magnetic property of h-Fe_2O_3 dramatically. Furthermore, it can be found that there are no evident changes in the coercivity from the enlarged view of the central loop of the h-Fe_2O_3 and h-Fe_2O_3@SiO_2-CD/Ag. The content of silver in h-Fe_2O_3@SiO_2-CD/Ag was also estimated by using ICP-AES analysis. Initially, the definite amount of catalyst was digested in concentrated hydrochloric and nitric acids solution. The resulting extract was then analyzed by ICP-AES. The Ag content was calculated as 0.4 w/w%.

Catalytic activity of nanomagnetic h-Fe_2O_3@SiO_2-CD/Ag

Considering the importance of the A^3 and KA^2 coupling reactions, the catalytic activity of the h-Fe_2O_3@SiO_2-CD/Ag was studied for promoting these reactions. Initially, reaction of benzaldehyde, phenyl acetylene and morpholine was selected as a model reaction and carried out in the presence of catalytic amount of the catalyst (20 mg) under conventional reflux condition in aqueous media.

The results established high catalytic activity of the h-Fe_2O_3@SiO_2-CD/Ag (90%). Motivated by this result and in attempt to achieve a green and rapid procedure, the model reaction was performed under ultrasonic irradiation. Gratifyingly, the desired product was furnished in high yield (97%) in a very short reaction time. According to the previous reports,[16,27] we define the efficiency of ultrasound irradiation on the base of cavitation phenomena. That is, formation, growth and collapse of the cavities which result in generation of high local temperatures and pressures. These can concentrate huge amount of energy from the conversion of kinetic energy of liquid motion into heating of the contents of the cavities. This can be considered as a driving force for promoting the organic transformation.[27] It is proved that the ultrasonic irradiation not only can accelerate the reaction rate, but also affect the reaction through altering the reaction pathway and enhancing chemical reactivity. Subsequently, to elucidate whether the extract-based reduction of the silver species can affect the catalytic activity, the catalytic activity of h-Fe_2O_3@SiO_2-CD/Ag was compared with that of h-Fe_2O_3@SiO_2-CD/Ag–H (in which the silver was reduced by hydrazine). Interestingly, h-Fe_2O_3@SiO_2-CD/Ag–H exhibited comparative catalytic activity. This result established that both chemical reduction and extract-based reduction can lead to the catalysts with high catalytic activity. Hence, both preparation procedures can be chosen. When the green chemistry is of focus, the green-synthesis approach is privileged while using commercially available hydrazine as the reduction agent can render chemical reduction more feasible.

According to the literature, the Ag(0) NPs is the dominant catalytic active site for promoting A^3 coupling reaction.[28–31] Ag(0) NPs can activate the substrate (phenyl acetylene) and promote formation of intermediates which then transformed into the desired product (see Reaction mechanism section). Hence, it can be concluded that the content of Ag(0) NPs can influence the catalytic activity. To confirm this postulation, h-Fe_2O_3@SiO_2-CD/Ag with various content of Ag(0) (0.2–0.8 w/w%) were synthesized and their catalytic activities were compared. It was found that small amount of silver can catalyse the reaction efficiently. Therefore, the need for scant amount of silver can be considered as the merit of this protocol. Moreover, it was found that increasing the amount of silver content from 0.2 to 0.4 w/w% can improve the catalytic activity. This can be attributed to

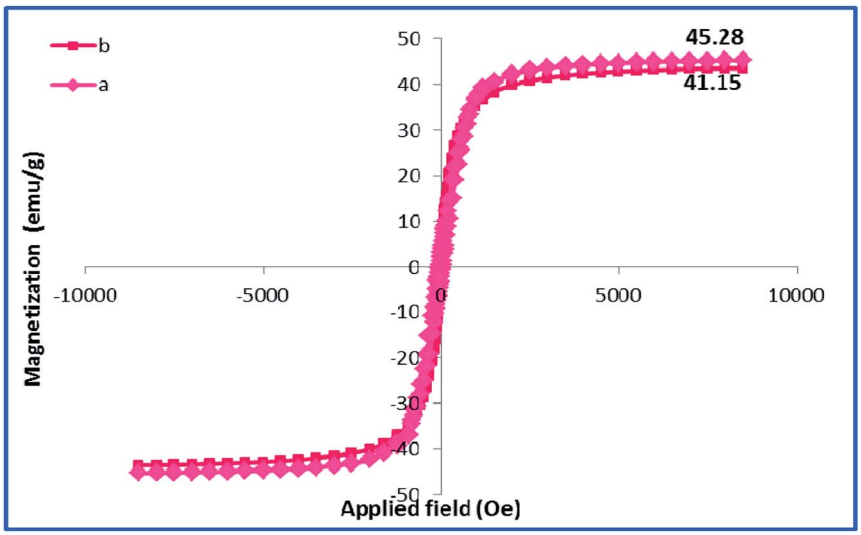

Fig. 7 VSM analyses of (a) h-Fe_2O_3 and (b) h-Fe_2O_3@SiO_2-CD/Ag.

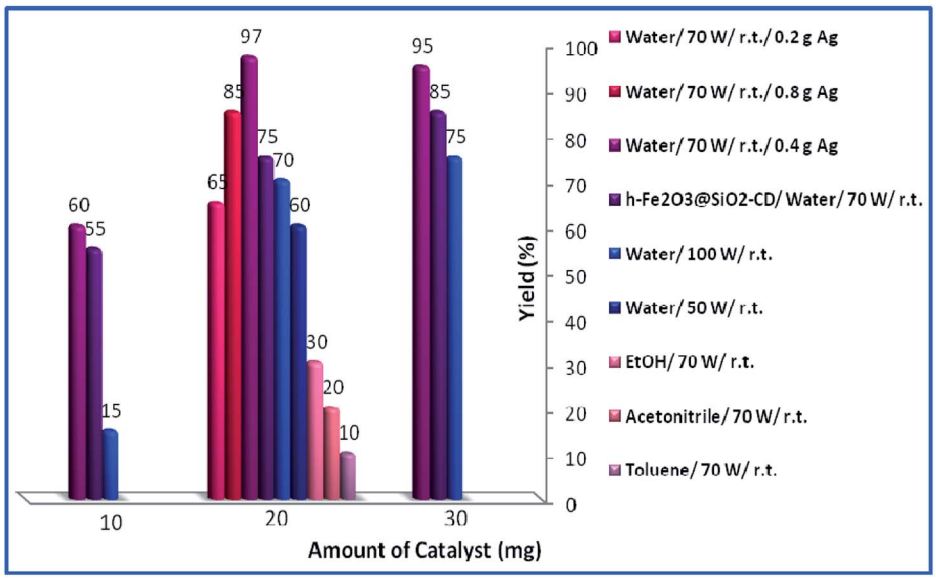

Fig. 8 Effects of loading of catalyst, duration of reaction and solvent for the synthesis of propargylamine.

the increase of the catalytic active sites. However, this trend was not sustainable and further increase of silver content not only did not improve the catalytic activity but also had a detrimental effect on the catalytic performance. This observation can be attributed to the aggregation of the Ag(0) NPs aggregation.

To explore the role of CD in the catalytic activity, the catalytic activity of h-Fe_2O_3@SiO_2-CD/Ag was compared with that of Fe_2O_3@SiO_2–N_2/Ag. The result clearly demonstrated the superior catalytic activity of the former, indicating the effective role of CD in the catalytic activity. According to the literature, this observation can be attributed to the NPs and CD.[32] Moreover, it is postulated that the presence of the CD can stabilize the NPs.[33]

Then, the reaction variables including ultrasonic irradiation, solvent and catalyst amount were optimized by altering the reaction variables and studying their effects on the yield of the model product (Fig. 8). As shown in Fig. 8, increasing the amount of catalyst from 10 mg to 20 mg resulted in higher yields. However, dependent on the reaction condition, more increase in the catalyst amount (to 30 mg) had different effects on the yield of the product. As depicted, in toluene, acetonitrile and EtOH, this had a detrimental effect on the yield of the reaction and no product was obtained using 30 mg catalyst. This can be assigned to the formation of various by-products. In the case of water as a solvent, the effect of the catalyst amount is influenced by the power of the used ultrasonic irradiation. Using 30 mg catalyst under low (50 W) or high (100 W) power of ultrasonic irradiation resulted in increase of the yield of the product while using medium (70 W) ultrasonic power reduced the yield slightly. The optimum reaction variables were found to be using 20 mg catalyst under ultrasonic irradiation of power 70 W in aqueous media and ambient temperature.

Having the optimum reaction condition in hand, the generality of this protocol was examined by using various amines and aldehydes with different electron densities (Table 2). As shown in this table, aldehydes with both electron donating and electron withdrawing functional groups could furnish the corresponding products in high yields. However, using heterocyclic aldehyde, furfural, led to slightly lower yield. These results established the reliability of this protocol. Encouraged by these results, we studied the possibility of replacing aldehydes with ketones, KA^2 coupling reaction (Table 2, products **4r** and **4s**). Interestingly, h-Fe_2O_3@SiO_2-CD/Ag could also catalyse this reaction to furnish the corresponding products in high yields. Finally, the efficiency of this protocol and the catalytic performance of h-Fe_2O_3@SiO_2-CD/Ag for catalysing the model reaction were compared with those of some previously reported catalytic methodologies to disclose the merits of this procedure (Table 3). As obvious, h-Fe_2O_3@SiO_2-CD/Ag resulted in desired product in higher or comparative yields. However, compared to all cases, h-Fe_2O_3@SiO_2-CD/Ag led to the product in shorter reaction time. Moreover, the presented protocol does not required any harsh reaction condition, inert atmosphere or toxic solvent.

Reaction mechanism

Considering the previous reports,[14,34] the plausible mechanism for the formation of propargylamines includes activation of terminal C–H bond of phenylacetylene by Ag NPs of the catalyst and formation of an intermediate, Ag–acetylide I. In this regard the suggested mechanism involves the activation of the C–H bond of alkyne *via* interaction by the metal nanoparticles (M). Thus, terminal alkyne is converted into the M···acetylide intermediate (I). The nucleophilic addition of the amine to the already activated aldehyde by Ag leads to generation of iminium ion (II). Next, the M···acetylide intermediate attacks the iminium ion simultaneously to provide the corresponding propargylamine (III). In this process one molecule of water can be formed from hydroxyl group and hydrogen of terminal alkyne, Scheme 2.

Table 2 Synthesis of three-component reaction of derivatives aldehyde or cyclic ketone, secondary-amines and terminal alkynes[a3,14,34–36]

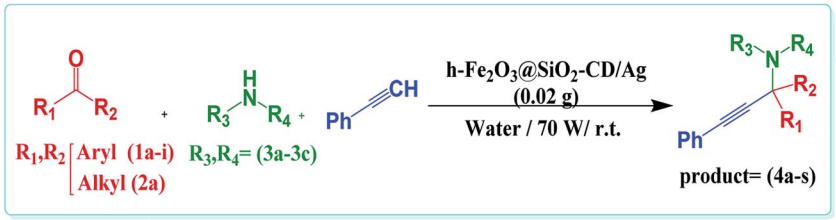

R^1	R^2	R^3	R^4	Product	Time (min)	Yield[b] (%)
1a: C_6H_5	H	**3a:** $-(CH_2)_5-$		**4a**	7	97
1b: *p*-Cl–C_6H_4	H	**3a**		**4b**	10	95
1c: *p*-NO_2–C_6H_4	H	**3a**		**4c**	12	90
1d: *p*-Me–C_6H_4	H	**3a**		**4d**	15	90
1e: *p*-MeO–C_6H_4	H	**3a**		**4e**	8	91
1f: *o*-OH–C_6H_4	H	**3a**		**4f**	10	94
1g: Furfuryl	H	**3a**		**4g**	12	85
1h: *p*-OHCC_6H_4	H	**3a**		**4h**	10	90
1a	H	**3b:** $-(CH_2)_2-O-(CH_2)_2-$		**4i**	8	97
1b	H	**3b**		**4j**	8	90
1c	H	**3b**		**4k**	12	85
1d	H	**3b**		**4l**	15	90
1e	H	**3b**		**4m**	10	92
1f	H	**3b**		**4n**	12	96
1g	H	**3b**		**4o**	20	90
1i: *m*-NO_2–C_6H_4	H	**3b**		**4p**	20	90
1a	H	**3c:** C_2H_5	C_2H_5	**4q**	15	88
2a: $-(CH)_5-$		**3a**		**4r**	20	89
2a		**3b**		**4s**	15	90

[a] Reaction conditions: aliphatic ketone **2a** (1.0 equiv.) or arylaldehydes **1a** (1.0 equiv.), amines **3a** (1.0 equiv.), alkynes (1.1 equiv.), H_2O (20 mL) and h-Fe_2O_3@SiO_2-CD/Ag (0.02 g) under ultrasonic irradiation (70 W) at room temperature. [b] Isolated yield.

Table 3 Comparison of h-Fe_2O_3@SiO_2-CD/Agwith other recently reported acid catalysts for the synthesis of propargylamine

Catalyst (amount)	Reaction conditions	Time (min)	Catalyst amount	Yield (%)	Ref.
CuI	H_2O/r.t./U.S	45	15 mg	98	37
h-Fe_2O_3@SiO_2-CD/Ag	H_2O/r.t./70 W	7	20 mg	97	This work
h-Fe_2O_3@DA/Ag	S.F./90 °C	60	10 mg	96	14
Gold nanocrystals stabilized on montmorillonite	Reflux/toluene	180	20 mg	91	38
ZnO nanoparticles	Stirrer/90 °C	120	10 mol%	89	5
Immobilized silver on surface-modified ZnONPs	Reflux/H_2O	240	10 mol%	89	30
Cu_2O–ZnO	S.F./100 °C	60	10 mg	95	35
CuCN	[bmim]PF_6/S.F./120 °C	120	2 mol%	95	39
CuNPs/TiO_2	Neat/70 °C	420	0.5 mol%	91	1
Nafion-NR50	CH_3CN/70–80 °C/N_2 atm	300	350 mg	85	40
ZnS	Reflux/CH_3CN	270	10 mol%	89	41

Catalyst reusability

The reusability of a heterogeneous catalyst is an important feature that makes it green and economically-efficient. To investigate the possibility of reusing h-Fe_2O_3@SiO_2-CD/Ag, the yields of the model reaction in the presence of fresh and reused catalysts in various time intervals were measured and compared, Fig. 9.

As shown in this figure, the catalyst can be recovered and reused for four times without any loss of catalytic activity. Reusing the catalyst for the fifth run, however, led to slight loss of catalytic activity. Upon reusing the catalyst for the sixth run, remarkable loss of catalytic activity (10%) was observed and the desired product was furnished in lower yield. To justify this behaviour, the leaching of Ag(0) NPs of reused catalysts were studied using hot filtration method and ICP-AES analysis. The results demonstrated zero leaching of Ag(0) NPs for the catalysts reused for four times. For the catalyst reused for fifth run only negligible loss of Ag(0) NPs was observed. This can justify the

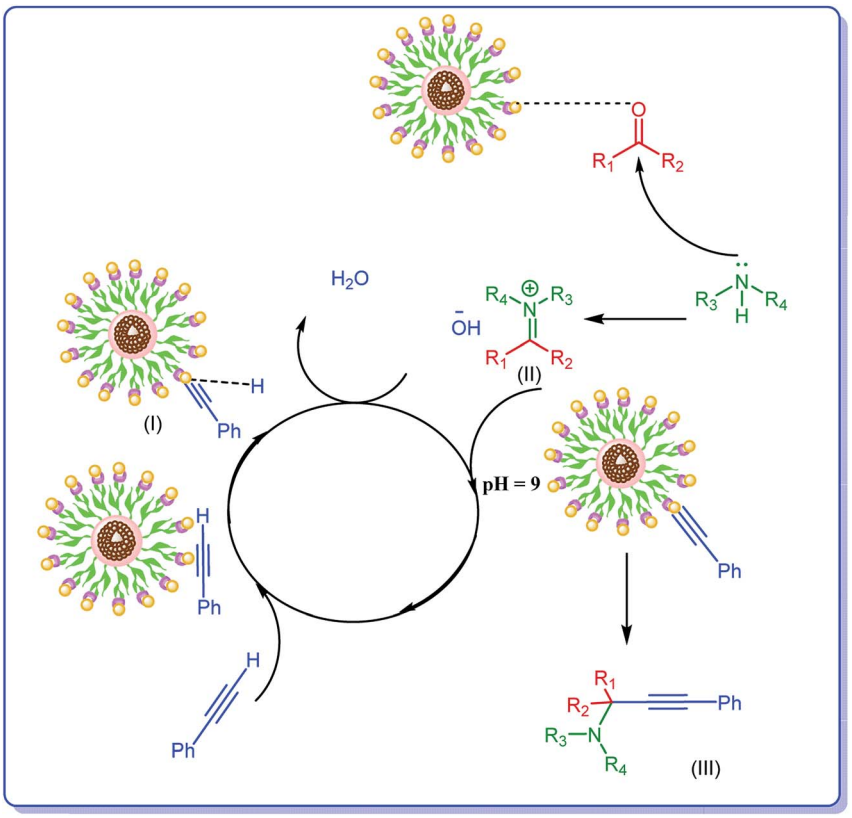

Scheme 2 Plausible mechanism for the synthesis of propargylamine catalyzed by h-Fe_2O_3@SiO_2-CD/Ag.

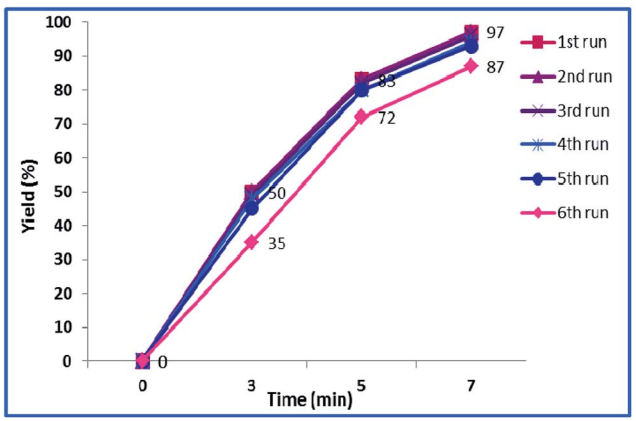

Fig. 9 Reusability of the h-Fe_2O_3@SiO_2-CD/Ag catalyst in A^3 coupling.

slightly lower catalytic activity of this catalyst. The leaching of Ag(0) NPs for the catalyst reused for sixth run however, were detectable. This finding can prove that the Ag(0) NPs are the catalytically active species. Moreover, the nature of the catalysis is heterogeneous.

Experimental

Materials and instruments

All chemicals and reagents, including trisodium citrate dihydrate, sodium acetate trihydrate, $FeCl_3 \cdot 6H_2O$, TEOS, β-cyclodextrin, *N*-(2-(trimethoxysilyl)ethyl)methanediamine, toluene, triethylamine, acetone, ethanol, ethylene glycol (EG), urea, $AgNO_3$, $NH_3 \cdot H_2O$ and hydrazine hydrate were analytical grade reagents, purchased from Sigma-Aldrich, and used without further purification. The progress of the organic reactions were monitored by TLC on commercial aluminum-backed plates of silica gel 60 F254, visualized, using ultraviolet light. Melting points were determined in open capillaries using an Electrothermal 9100 without further corrections. ^{1}H NMR and ^{13}C NMR spectra were recorded on Bruker DRX-400 spectrometer at 400 and 100 MHz respectively.

The catalyst characterization was performed by using various characterization techniques including XRD, FTIR, BET, SEM/EDX, TGA, and ICP-AES. FTIR spectra were obtained by using PERKIN-ELMER-Spectrum 65 instrument. The BET analyses were carried out using BELSORP Mini II instrument. Prior to BET analyses, the samples were degassed at 423 K for 3 h. SEM/EDX images were recorded by employing a Tescan instrument, using Au-coated samples and acceleration voltage of 20 kV. Room temperature powder X-ray diffraction patterns were obtained by using a Siemens, D5000. CuKα radiation from a sealed tube.

All compounds were known and were identified by comparison of their physical and spectroscopic data with those of authentic compounds and were found identical. However, we compared all compounds by their melting points. ^{1}H and ^{13}C NMR spectra of selected compounds are reported and given as ESI.†

Synthesis of nanomagnetic Fe_2O_3 hollow sphere (a)

Nanomagnetic Fe_2O_3 hollow sphere were prepared through solvothermal method.[14] Initially, $FeCl_3 \cdot 6H_2O$ (5 mmol) was dissolved in 70 mL of ethylene glycol in a flask. Next, 30 mmol of sodium acetate trihydrate, 1.5 mmol of trisodium citrate dehydrate and urea (17 mmol) were added to the aforementioned solution. The resulting mixture was stirred vigorously for 60 minutes and then, transferred to the Teflon-lined stainless-steel autoclave (150 mL capacity) and kept at 220 °C for 24 h. Upon completion of the process, the reactor was cooled to room temperature and the resulting brown product **1** was washed for three times with EtOH/H_2O and dried at 80 °C for 24 h in oven.

Synthesis of h-Fe_2O_3@SiO_2 core–shell NPs (b)

The h-Fe_2O_3@SiO_2 core–shell NPs was prepared according to a previously reported method with little modification.[42] Briefly, h-Fe_2O_3 (1 g) was dispersed in a mixture of 20 mL of deionized water, 50 mL of ethanol and 6 mL of NH_3. The pH value of the suspension was kept at *ca.* 11 and then, the mixture was sonicated for 30 min at room temperature. After that, TEOS (2 g) was added into the mixture, which was continuously stirred for 12 h at room temperature in air. Finally, the obtained h-Fe_2O_3@SiO_2 core–shell, **2**, was collected by an external magnet, washed three times with EtOH/H_2O to remove blank silica, and dried at 80 °C for 12 h in oven.

Synthesis of h-Fe_2O_3@SiO_2–N_2 core–shell NPs (c)

For amine-functionalization of the surface of h-Fe_2O_3@SiO_2-core–shell (h-Fe_2O_3@SiO_2) (3 g), was dispersed by sonication in 100 mL dry toluene for 1 h. Subsequently, 3-*N*-(2-(trimethoxysilyl)ethyl)methanediamine (3 mL) as functionalization group and Et_3N (3 mL) as a catalyst were added and the reaction mixture was refluxed overnight. At the end of the reaction, the mixture was cooled to room temperature and the amine-functionalized h-Fe_2O_3@SiO_2core–shell, **3**, was collected by using an external magnet and washed with toluene, and then dried under air for 12 h.

Synthesis of β-cyclodextrin-OTs (d)

Tosylation of CD with *p*-toluenesulfonyl chloride was performed according to literature procedure.[43] Typically, *p*-toluenesulfonylchloride (7.9 mmol) was added to a solution of pyridine containing 15.86 mmol of CD. The mixture was cooled to 0 °C and kept for 48 h. Upon completion, distilled water was added to the mixture and the solvent was evaporated to afford an oily product. The latter transformed into a white precipitate upon addition of cold water. The final product was achieved by filtration, recrystallization from water and drying.

Synthesis of h-Fe_2O_3@SiO_2-CD (e)

To synthesize the h-Fe_2O_3@SiO_2-CD, β-cyclodextrin-OTs (0.5 g) was dispersed in dry toluene (20 mL) under stirring condition. The pH value of the suspension was kept at *ca.* 7–8. Then, the resulting mixture was added to the suspension of h-Fe_2O_3@-SiO_2–N_2 core–shell **3** (1 g) in 20 mL dry toluene. After that, the suspension was heated under reflux condition overnight. Upon completion of the reaction, the brown product **5** was magnetically collected, washed with dry toluene for three times and dried in oven at 80 °C for 12 h.

Preparations of hollyhocks flower extract (f)

Fresh leaves of hollyhock flower were collected around Banaruiyeh District, in Larestan, Iran. First, the collected hollyhock flowers (2 g) were crushed in porcelain mortar. Then, the resulting powder was mixed thoroughly with 100 mL deionized water and boiled for 60 min at 80 °C. The extract **6** was obtained by cooling the mixture and simple filtration.

Extract-based synthesis of Ag NPs and their embedding into h-Fe_2O_3@SiO_2-CD: synthesis of h-Fe_2O_3@SiO_2-CD/Ag (g)

h-Fe_2O_3@SiO_2-CD (1 g) was dispersed into a solution of $AgNO_3$ (0.1 g) in 20 mL deionized H_2O under stirring condition at room temperature for 30 minutes. The Ag^+ ions were adsorbed onto the surfaces of h-Fe_2O_3@SiO_2-CD *via* the electrostatic attraction. After that the fresh extract **6** (1 mL) as a reducing agent was added into the suspension. Upon addition of the extract **6** the colour of the mixture was changed to black which indicate the reduction of silver to Ag(0). To immobilize Ag(0) NPs the into the h-Fe_2O_3@SiO_2-CD, the mixture was stirred for 12 h. Finally, the product **7** was successfully collected by magnetic separation, washed three times with EtOH/H_2O and dried at 60 °C for 12 h. The schematic processes of synthesis of the catalyst are depicted in Fig. 1. Notably, to compare the catalytic activity of the catalyst achieved from the extract-based approach with the one obtained from conventional chemical reduction of silver species, the immobilization of Ag(0) nanoparticles on h-Fe_2O_3@SiO_2-CD was also performed by reduction of silver precursor with hydrazine. To this purpose, the same procedure reported above was used except that the reduction was carried out by using 2 mL hydrazine hydrate. This catalyst was named as h-Fe_2O_3@SiO_2-CD/Ag–H. h-Fe_2O_3@SiO_2–N_2/Ag was also prepared through synthesis of h-Fe_2O_3@SiO_2–N_2 (c) and subsequent immobilization of Ag(0) NPs *via* extract-based approach similar to the one reported for the synthesis of h-Fe_2O_3@SiO_2-CD/Ag except that h-Fe_2O_3@SiO_2–N_2 was used as the starting material.

General procedure for A^3 and KA^2 coupling reactions

To a mixture of phenyl acetylene (1.1 equiv.), amine (1.0 equiv.), aldehyde or ketone (1.0 equiv.) in H_2O (10 mL) as a green solvent, nanomagnetic h-Fe_2O_3@SiO_2-CD/Ag (20 mg) was added. The mixture was subjected to ultrasonic irradiation of power of 70 W. The progress of the reaction was monitored by TLC. Upon completion of the reaction, the reaction mixture was cooled to ambient temperature and diluted with hot ethanol (10 mL). The catalyst was separated by an external magnet from the cooled mixture, washed with ethanol, dried in air and re-used for a consecutive reaction run under the same reaction conditions. The resulting residue was purified by recrystallization (hot ethanol) to obtain the excellent yield of product.

Spectral data of some selected compounds

1-(1,3-Diphenylprop-2-ynyl)piperidine (Table 2, 4a).[14] Pale yellow oily liquid; ^{1}H NMR (400 MHz, $CDCl_3$, ppm) δ 1.45–1.49 (m, 2H), 1.58–1.65 (m, 4H), 2.59 (t, 4H), 4.81 (s, 1H), 7.31–7.40 (m, 6H), 7.53–7.55 (m, 2H), 7.65–67 (d, J = 7.6 Hz, 2H).

1-(3-Phenyl-1-(4-(3-phenyl-1-(piperidin-1-yl)prop-2-ynyl)phenyl)-prop-2-ynyl)piperidine (Table 2, 4h).[14] White solid; mp 157–159 °C; ^{1}H NMR (400 MHz, $CDCl_3$, ppm) δ 1.47 (m, 2H), 1.59–1.63 (m, 4H), 2.59 (m, 4H), 4.81 (s, 1H), 7.33–7.35 (m, 3H), 7.52–7.55 (m, 2H), 7.63 (s, 2H).

***N*,*N*-Diethyl-1,3-diphenylprop-2-yn-1-amine (Table 2, 4q).**[14] Pale yellow oily liquid; ^{1}H NMR (400 MHz, $CDCl_3$, ppm) δ 1.04 (m, 6H), 2.36–2.62 (m, 4H), 5.19 (s, 1H), 7.15–7.27 (m, 4H), 7.29–7.38 (m, 3H), 7.39–7.41 (m, 2H).

4-(1-((4-Fluorophenyl)ethynyl)cyclohexyl)morpholine (Table 2, 4s).[14] Yellow oil; ^{1}H NMR (400 MHz, DMSO-d_6, ppm) δ 1.26–1.34 (m, 1H), 1.57–1.62 (m, 2H), 1.69–1.78 (m, 3H), 1.80–1.86 (m, 2H), 2.00–2.02 (m, 2H), 2.78 (s, 4H), 3.70 (br t, J = 4.2 Hz, 4H), 6.97–7.00 (t, J = 8.6 Hz, 2H), 7.32–7.40 (m, 2H).

Conclusions

In summary, hollyhock flower extract was used as a reducing agent for the synthesis of Ag(0) NPs on cyclodextrin decorated h-Fe_2O_3@SiO_2 core–shell, obtained through a green facile ultrasonic-assisted and template-free process, to furnish a novel and heterogeneous catalyst (h-Fe_2O_3@SiO_2-CD/Ag). The utility of the novel catalyst for catalyzingA^3 and KA^2 coupling reactions under mild and green condition, *i.e.* ultrasonic irradiation at room temperature in aqueous media was proved. Hot filtration experiments ruled out the remarkable Ag(0) leaching up to five reaction runs and the reused catalyst can be reused without negligible loss of catalytic activity.

Acknowledgements

The authors are thankful to Alzahra University Research Council S. Sadjadi and M. M. Heravi are also thankful to Iran National Science Foundation (INSF) for supporting this research under contract no. 95834576.

Notes and references

1 M. J. Albaladejo, F. Alonso, Y. Moglie and M. Yus, *Eur. J. Org. Chem.*, 2012, **2012**, 3093–3104.
2 G. Villaverde, A. Corma, M. Iglesias and F. Sanchez, *ACS Catal.*, 2012, **2**, 399–406.
3 S. V. Katkara and R. V. Jayaram, *RSC Adv.*, 2014, **4**, 47958–47964.
4 N. Salam, S. K. Kundu, A. Singha Roy, P. Mondal, S. Roy, A. Bhaumik and S. Manirul Islam, *Catal. Sci. Technol.*, 2013, **3**, 3303–3316.
5 K. V. V. Satyanarayana, P. Atchuta Ramaiah, Y. L. N. Murty, M. R. Chandra and S. V. N. Pammi, *Catal. Commun.*, 2012, **25**, 50–53.
6 B. J. Borah, S. J. Borah, K. l. Saikia and D. K. Dutta, *Catal. Sci. Technol.*, 2014, **4**, 4001–4009.
7 T. Zeng, W.-W. Chen, C. M. Cirtiu, A. Moores, G. Song and C.-J. Li, *Green Chem.*, 2010, **12**, 570–573.
8 G.-P. Yong, D. Tian, H.-W. Tong and S.-M. Liu, *J. Mol. Catal. A: Chem.*, 2010, **323**, 40–44.
9 X. Zhang, Y. Niu, Y. Yang, Y. Li and J. Zhao, *New J. Chem.*, 2014, **38**, 4351–4356.
10 N. E. A. El-Gamel, L. Wortmann, K. Arroubb and S. Mathur, *Chem. Commun.*, 2011, **47**, 10076–10078.
11 T. Georgelin, V. Maurice, B. Malezieux, J.-M. Siaugue and V. Cabuil, *J. Nanopart. Res.*, 2010, **12**, 675–680.
12 M. Shao-cong, W. Hong, Q. Ming, Q. Cheng-wu, Y. Yong and L. Yong-wang, *J. Fuel Chem. Technol.*, 2015, **43**, 692–700.
13 J. Zhu, Y. Shen, C. Yao and A. Xie, *Colloid J.*, 2016, **78**, 156–163.
14 A. Elhampour, M. Malmir, E. Kowsari, F. A. Boorboor and F. Nemati, *RSC Adv.*, 2016, **6**, 96623–96634.
15 Q. He, Z. Wu and C. Huang, *J. Nanosci. Nanotechnol.*, 2012, **12**, 2943–2954.
16 H. Naeimi and R. Shaabani, *Ultrason. Sonochem.*, 2017, **34**, 246–254.
17 M. Navid and S. Rad, *Ultrason. Sonochem.*, 2017, **34**, 865–872.
18 S. Sadjadi, M. M. Heravi and M. Daraie, *J. Mol. Liq.*, 2017, **231**, 98–105.
19 S. Sadjad, M. M. Heravi and M. Daraie, *Res. Chem. Intermed.*, 2017, **43**, 843–857.
20 M. M. Heravi, E. Hashemi, Y. Shirazi Beheshtiha, S. Ahmadi and T. Hosseinnejad, *J. Mol. Catal. A: Chem.*, 2014, **394**, 74–82.
21 M. M. Heravi, F. Mousavizadeh, N. Ghobadi and M. Tajbakhsh, *Tetrahedron Lett.*, 2014, **55**, 1226–1228.
22 S. Sadjadi, M. M. Heravi and M. Daraie, *Res. Chem. Intermed.*, 2017, **43**, 2201–2214.
23 F. Benakashani, A. R. Allafchian and S. A. H. Jalali, *Int. J. Mod. Eng. Sci.*, 2016, **2**, 251–258.
24 C. Cannas, A. Musinu, G. Navarra and G. Piccaluga, *Phys. Chem. Chem. Phys.*, 2004, **006**, 3530–3534.
25 P. Yuan, P. D. Southon, Z. Liu, M. E. R. Green, J. M. Hook, S. J. Antill and C. J. Kepert, *J. Phys. Chem. C*, 2008, **112**, 15742–15751.
26 S. Kumar-Krishnan, A. Hernandez-Rangel, U. Pal, O. Ceballos-Sanchez, F. J. Flores-Ruiz, E. Prokhorov, O. Arias de Fuentes, R. Esparza and M. Meyyappan, *J. Mater. Chem. B*, 2016, **4**, 2553–2560.
27 S. Sadjadi and M. Eskandari, *Ultrason. Sonochem.*, 2013, **20**, 640–643.
28 N. Salam, S. K. Kundu, R. A. Molla, P. Mondal, A. Bhaumik and S. M. Islam, *RSC Adv.*, 2014, **4**, 47593–47604.
29 M. Trose, M. Dell'Acqua, T. Pedrazzini, V. Pirovano, E. Gallo, E. Rossi, A. Caselli and G. Abbiati, *J. Org. Chem.*, 2014, **79**, 7311–7320.
30 F. Movahedia, H. Masrouria and M. Z. Kassaee, *J. Mol. Catal. A: Chem.*, 2014, **395**, 52–57.
31 M. Jeganathan, A. Dhakshinamoorthy and K. Pitchumani, *Sustainable Dev. Chem. Eng.*, 2014, **2**, 781–787.

32 H. Wu, H. Liu, W. Yang and D. He, *Catal. Sci. Technol.*, 2016, **6**, 5631–5646.
33 C. Putta, V. Sharavath, S. Sarkar and S. Ghosh, *RSC Adv.*, 2015, **5**, 6652–6660.
34 L. Shi, Y.-Q. Tu, M. Wang, F.-M. Zhang and C.-A. Fan, *Org. Lett.*, 2004, **6**, 1001–1003.
35 M. S. Hosseini and F. Moeini, *New J. Chem.*, 2014, **38**, 624–635.
36 M. Tajbaksh, M. Farhang, H. R. Mardani, R. Hosseinzadeh and Y. Sarrafi, *Chin. J. Catal.*, 2013, **34**, 2217–2222.
37 B. Sreedhar, P. R. Surendra, B. P. Veda and A. Ravindra, *Tetrahedron Lett.*, 2005, **46**, 7019–7022.
38 B. Jyoti Borah, S. Jyoti Borah, K. Saikia and D. Kumar Dutta, *Catal. Sci. Technol.*, 2014, **44**, 4001–4009.
39 S. B. Park and H. Alper, *Chem. Commun.*, 2005, 1315–1317, DOI: 10.1039/b416268d.
40 M. Kidwai and A. Jahan, *J. Iran. Chem. Soc.*, 2011, **8**, 462–469.
41 N. P. Eagalapati, A. Rajack and Y. L. N. Murthy, *J. Mol. Catal. A: Chem.*, 2014, **381**, 126–131.
42 T. K. H. Ta, M.-T. Trinh, N. V. Long, T. T. M. Nguyen, T. L. T. Nguyen, T. L. Thuoc, B. T. Phan, D. Mott, S. Maenosono, H. Tran-Van and V. H. Le, *Colloids Surf., A*, 2016, **504**, 1–8.
43 B. Martel, Y. Leckchiri, Y. Alain Pollet and M. Morcellet, *Eur. Polym. J.*, 1995, **31**, 1083–1088.